

# Reports

## Atomic Images by Electron-Wave Holography

**Abstract.** *Direct views of electron clouds in atoms have been observed visually and photographed by means of a two-stage holographic microscope based on Gabor's principle of image reconstruction. Holograms are produced with 40-kilo-volt electron radiation and decoded with an optical laser. The obviation of an objective lens makes feasible a numerical aperture of 0.37 and a resolving power exceeding 0.1 angstrom.*

The sizes and shapes of electron clouds in atoms have been known for a half century from inferences based on experimental x-ray studies (1) and theoretical quantum calculations (2). Despite general acceptance of the correctness of this information, the direct observation of atoms has remained an intriguing goal. Two decades ago Müller successfully resolved atomic images with his field-electron (3) and field-ion (4) microscopes, and subsequently more conventional electron microscopes with this capability have been developed (5). Although the micrographs are remarkable, the resolving power has been insufficient to permit characterization of the spatial distributions of the planetary electrons orbiting the atomic nuclei.

The key to improving the resolving power of electron microscopes was pointed out by Gabor (6) in 1948. Gabor formulated the principle of holography, whereby information on the phase as well as the amplitude of a wave emanating from an object is recorded on a photographic plate (the hologram) by coherent superposition of the object wave upon a strong refer-

ence wave prior to recording. A facsimile of the wave front from the original object can be reconstructed in a second optical stage if the hologram is used as an intricate diffraction grating. Indeed, Gabor explicitly suggested the possibility of a two-stage holographic microscope of enormous power employing electron waves ( $\lambda_1 \approx 5 \times 10^{-2}$  Å) in the first stage and visible light ( $\lambda_2 \approx 5 \times 10^3$  Å) in the second. A magnification proportional to  $\lambda_2/\lambda_1 \approx 10^5$  could be achieved without the agency of an objective lens, the weakest

feature of conventional microscopes in view of the severe spherical aberration characteristic of electron lenses.

Taking advantage of Gabor's idea, we have designed and successfully operated a microscope in which the theoretical resolving power is 0.08 Å under normal operating conditions with  $\lambda_1 = 0.06$  Å and a numerical aperture of 0.37. This resolving power is nearly two orders of magnitude higher than that of conventional electron microscopes. Heretofore, the impediment frustrating the realization of such performance in holographic microscopes has been the lack of a method for producing a suitable wide-angle reference wave of electrons coherent with the object waves. The unattainability of electron lasers rules out techniques similar to those of optical holography. However, in the case of the objects of particular interest to us, the electron clouds of atoms, the solution of the problem turned out to be simple. When electron waves in the first stage of the microscope encounter atoms in a gaseous sample, they are weakly scattered by the individual atomic electrons but strongly scattered by the atomic nuclei (Rutherford scattering). It is possible to use the latter component of the scattered waves as a reference wave for the coherent component of the former. Each atom, as it were, is able to produce its own refer-

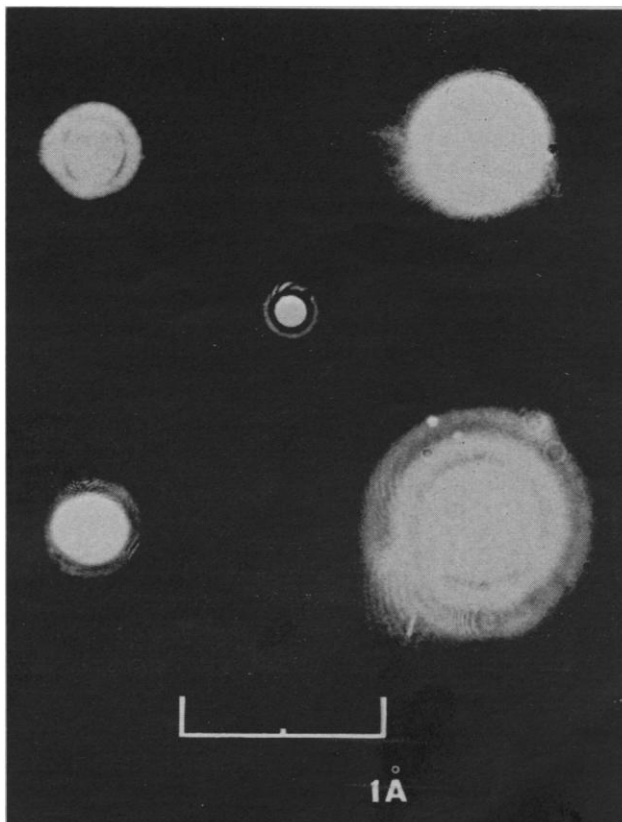


Fig. 1. Holographic micrographs of electron densities in atomic neon (top) and argon (bottom) at 260,000,000 power. Short (left) and long (right) exposures are reproduced. Shown in the center is the Airy diffraction pattern corresponding to the operating wavelength, numerical aperture, and magnification. Its disk of confusion limits the resolving power and its odd-numbered bright rings (minima in the Airy amplitudes) are associated with the dark rings in the atomic images. It must be emphasized, accordingly, that the diffuse rings in the atomic photographs are intrinsic instrumental diffraction effects and are not due to the atomic shell structure. See Figs. 2 and 3. No physical significance should be attributed to speckles and deviations from circular symmetry.

**Scoreboard for Reports:** In the past few weeks the editors have received an average of 68 Reports per week and have accepted 12 (17 percent). We plan to accept about 12 reports per week for the next several weeks. In the selection of papers to be published we must deal with several factors: the number of good papers submitted, the number of accepted papers that have not yet been published, the balance of subjects, and length of individual papers.

Authors of Reports published in *Science* find that their results receive good attention from an interdisciplinary audience. Most contributors send us excellent papers that meet high scientific standards. We seek to publish papers on a wide range of subjects, but financial limitations restrict the number of Reports published to about 15 per week. Certain fields are overrepresented. In order to achieve better balance of content, the acceptance rate of items dealing with physical science will be greater than average.

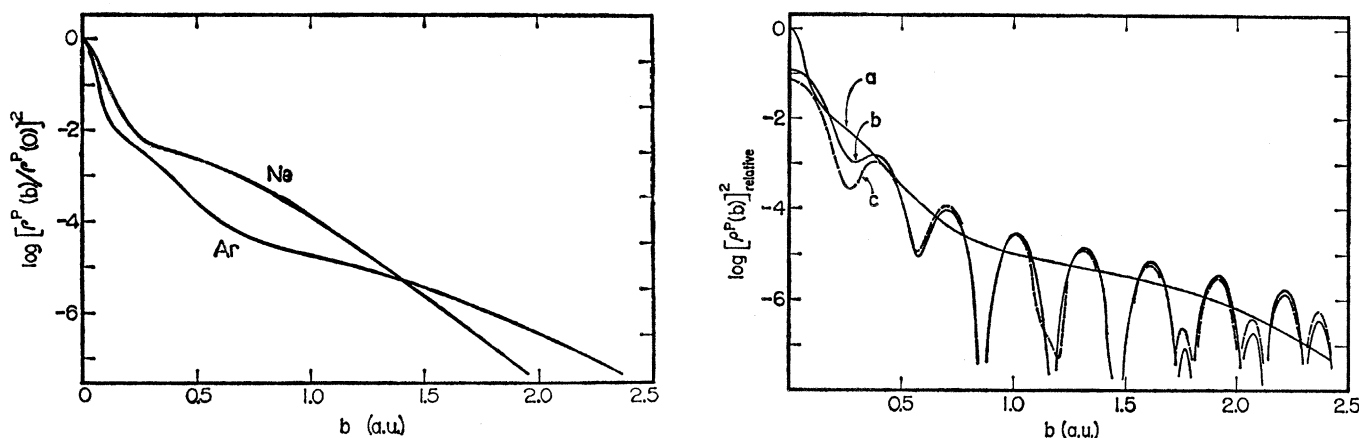


Fig. 2 (left). Logarithmic plots of the quantum-theoretical image intensities,  $[\rho^P(b)]^2$ , at infinite resolving power for neon and argon atoms as a function of  $b$ , the distance in atomic units (1 a.u. = 0.53 Å) of the line of sight from the atomic center. Fig. 3. Logarithmic plots of calculated image intensities of the electron cloud in argon as a function of distance from the atomic center. (Curve a) Square of the projected electron density. (Curve b) Image intensity of an ideal micrograph imaging only the radiation scattered coherently by the electron cloud. The undulations are diffraction effects associated with a numerical aperture of 0.37 and a wavelength of 0.06 Å and are *not* to be associated with atomic shell structure. In the limit of vanishing wavelength or large numerical aperture, or both, this curve would approach curve a. (Curve c) Calculated holographic reconstruction intensity for a numerical aperture of 0.37, a wavelength of 0.06 Å, and a limiting holographic absorbance of 2.0 at the periphery, including the degradative influence of the undiffracted wave from the reconstruction beam at the image center.

ence wave, and the sum of the emergent waves from atoms, when suitably filtered by a rotating sector, is recorded on a photographic plate to obtain a hologram. Each atom generates its own hologram, but, since all holograms are recorded at the Fraunhofer diffraction limit and centered on a common origin, all atomic images are exactly centered on top of each other. The twin images from the Fourier holograms of the spherical objects are also superposed upon each other. The reconstruction is not degraded by the above superpositions because the images are all identical if the sample is a pure monatomic gas. Since the final image is the average of an ensemble, each individual member need suffer only one incident quantum of radiation and radiation damage is therefore insignificant. Nevertheless, the electronic excitation induced by this one quantum does lead to a background of incoherent scattering which washes out reconstructed images by a small and readily calculable extent. The possibility exists of obtaining some molecular information by an approach analogous to the above technique if the molecules contain a heavy atom to provide a reference wave for surrounding atoms.

For the first stage of our apparatus we used a gas-phase electron diffraction unit described elsewhere (7), equipping it with a rotating sector with an angular opening proportional to  $\sin^4(\theta/2) \sec^3\theta$ , where  $\theta$  is the angle of scattering of the electrons. This filter compensates for the Rutherford attenuation of scat-

tered intensity with increasing  $\theta$ , and for the inverse square law and angle of incidence of electrons as they encounter the flat photographic plate. The holograms are then reduced severalfold, for convenience, on Polaroid positive transparencies and placed in the second stage of our device, a helium-neon laser diffractometer, the principal component of which is an  $f/15$  lens with a focal length of 114 cm. The temporal coherence requirements in the reconstruction stage are so modest that a laser is used for convenience, not because of necessity. The Fraunhofer diffraction pattern arising when monochromatic light passes through the hologram is a reconstructed image of the electronic distribution in the atoms under scrutiny. Images are distorted by the usual factors encountered in holography, the nonnegligible contribution from the square of the amplitude of the object waves, the incoherent scattering, and degradation of information in photographic processes.

Images may be viewed or photographed through the eyepiece of the diffractometer. Figure 1 reproduces images of neon and argon atoms so obtained, at 260,000,000 diameters. The diffuse rings are *not* electron shells but are intrinsic instrumental effects. See the captions of Figs. 1 through 3 for details.

Except for distortions characteristic of holography (provided that the holographic blackening is proportional to electron intensity), the amplitude of the reconstruction in the second stage can

be shown to correspond to the projected electron density  $\rho^P(b)$  of an atom, that is, the density integrated from the back to the front of an atom along a line of sight at a distance  $b$  from the nucleus. The intensity of the image, then, represents the square of the projected density. For the sake of comparison with the experimental images we portray the behavior of  $[\rho^P(b)]^2$  in Fig. 2 as deduced from the quantum-theoretical wave functions of Clementi and Raimondi (8). The falloff of  $[\rho^P(b)]^2$  is so precipitous that a logarithmic rather than linear representation is necessary if any hint of the atomic shell structure is to be perceived visually. Chemists often acquire an exaggerated mental image of the sharpness of electron shells that is inconsistent with the evidence embodied in Fig. 2. Also illustrated in Fig. 2, with its ordinate representing a variation of more than six orders of magnitude, is the difficulty associated with reproducing atomic images faithfully by photographic means.

Although the technique presented here makes possible a spectacular increase in resolving power, it is simple to apply only in the case of a severely limited class of specimens. Within this limitation it is straightforward and effective. It has supplied the most direct views of electronic clouds in atoms obtained to date.

L. S. BARTELL  
C. L. RITZ

Department of Chemistry,  
University of Michigan,  
Ann Arbor 48104

## References and Notes

1. Key references include W. L. Bragg, R. W. James, C. H. Bosanquet, *Phil. Mag.* **44**, 433 (1922); R. J. Havighurst, *Phys. Rev.* **29**, 1 (1927); E. O. Wollan, *ibid.* **38**, 15 (1931). Corresponding studies by electron diffraction were first reported by L. S. Bartell and L. O. Brockway [*Phys. Rev.* **90**, 833 (1953)].
2. E. Schrödinger, *Ann. Phys. (Leipzig)* **79**, 361 (1926); D. R. Hartree, *Proc. Cambridge Phil. Soc.* **24**, 89 (1928); *ibid.*, p. 111; *ibid.*, p. 426.
3. E. W. Müller, *Z. Naturforsch. A* **5**, 473 (1950).
4. —, *J. Appl. Phys.* **27**, 474 (1956).
5. See, for example, A. V. Crewe, J. Wall, J. Langmore, *Science* **168**, 1338 (1970); F. P. Ottensmeyer, E. E. Schmidt, A. J. Olbrecht, *ibid.* **179**, 175 (1973).
6. D. Gabor, *Nature (Lond.)* **161**, 777 (1948); *Proc. Roy. Soc. London Ser. A* **197**, 454 (1949).
7. L. S. Bartell, in *Techniques of Chemistry: Physical Methods in Chemistry*, A. Weissberger and B. W. Rossiter, Eds. (Interscience, New York, ed. 4, 1972), vol. 1, part 3D, pp. 125–158.
8. E. Clementi and D. L. Raimondi, *J. Chem. Phys.* **38**, 2686 (1963).
9. This work was supported by a grant from the National Science Foundation.
- 6 May 1974

## Stratospheric Ozone Destruction by Man-Made Chlorofluoromethanes

**Abstract.** Calculations indicate that chlorofluoromethanes produced by man can greatly affect the concentrations of stratospheric ozone in future decades. This effect follows the release of chlorine from these compounds in the stratosphere. Present usage levels of chlorofluoromethanes can lead to chlorine-catalyzed ozone destruction rates that will exceed natural sinks of ozone by 1985 or 1990.

Chlorofluoromethanes ( $\text{CF}_x\text{Cl}_y$ ), principally  $\text{CF}_2\text{Cl}_2$  and  $\text{CFCl}_3$ , are being produced as aerosol propellants and refrigerants in large and growing amounts, and their atmospheric concentrations are increasing (1–3). These compounds have been considered valuable as tracers of atmospheric motions because they are relatively inert chemically with atmospheric lifetimes exceeding 10 years (4). Unlike  $\text{CCl}_4$  (1), they seem to have no natural sources or sinks in the troposphere; their lifetimes are controlled by diffusion into the stratosphere where they can be photodissociated by ultraviolet light (5). Molina and Rowland (5) have noted that this stratospheric sink for  $\text{CF}_x\text{Cl}_y$  also represents a potential sink for stratospheric  $\text{O}_3$ . This is so because the photodissociation of  $\text{CF}_x\text{Cl}_y$  releases chlorine atoms which can catalytically destroy  $\text{O}_3$  through reactions like those of the nitrogen oxides ( $\text{NO}_x$ ) with  $\text{O}_3$  (5–8). Because of the great importance of stratospheric  $\text{O}_3$  (9), we have reexamined this potential effect and its likely time evolution. We find that current  $\text{CF}_x\text{Cl}_y$  usage levels and trends can lead to chlorine-catalyzed  $\text{O}_3$  destruction rates exceeding all natural sinks of stratospheric  $\text{O}_3$  by the early 1980's. Stratospheric changes will continue long after ground-level emissions cease. For example, if emissions were curtailed now, the resultant  $\text{O}_3$  destruction would maximize around 1990 and would remain significant for several decades. Our calculations also indicate that the  $\text{Cl}_x$  concentrations (the sum of the concentrations of  $\text{Cl}$ ,  $\text{ClO}$ , and  $\text{HCl}$ ) will increase significantly in the stratosphere but not in the troposphere.

Hence, critical monitoring of this problem will require measurements in the stratosphere; tropospheric observations alone will not suffice.

After release,  $\text{CF}_x\text{Cl}_y$  molecules diffuse upward to be photolyzed by solar radiation (chiefly 175- to 220-nm ultraviolet wavelengths) in the stratosphere. On the basis of several atmospheric measurements (1–3) and known chemical properties of the chlorofluoromethanes, stratospheric photolysis ap-

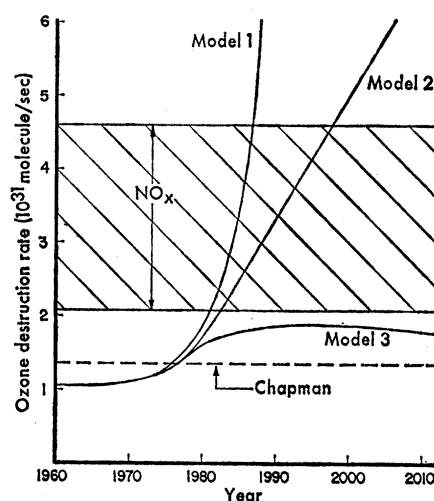
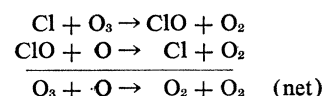


Fig. 1. Globally integrated  $\text{O}_3$  destruction rates for three model time histories of  $\text{CF}_x\text{Cl}_y$  emission. Corresponding rates appear for the natural  $\text{O}_3$  sinks due to pure oxygen (labeled "Chapman") reactions and  $\text{NO}_x$  reactions. The width of the  $\text{NO}_x$  band is due mostly to a lack of knowledge of the natural  $\text{NO}_x$  abundance and altitude distribution. All quantities were computed on the basis of present-day atmospheric background and have been integrated to 60-km altitude. The stratospheric  $\text{O}_3$  production rate, integrated globally, is about  $6 \times 10^{31} \text{ sec}^{-1}$ . Above 50 km the hydrogen oxides can also destroy  $\text{O}_3$ .

pears to be the major sink for  $\text{CF}_x\text{Cl}_y$  (5). Several other possible sinks have been suggested but appear to be negligible (10). After release of the first chlorine atom by a solar photon, chemical reactions will probably remove the remaining chlorine and fluorine atoms from the  $\text{CF}_x\text{Cl}_{y-1}$  radical, temporarily forming phosgene-type molecules (5). Once free in the stratosphere, chlorine atoms can catalyze the recombination of  $\text{O}_3$  and atomic oxygen. The key reaction are (5–8)



Eventually, the chlorine released from  $\text{CF}_x\text{Cl}_y$  should reach the ground through downward diffusion and tropospheric rainout (6–8).

We have quantitatively estimated globally averaged rates of  $\text{O}_3$  destruction due to the chlorine atoms released in the initial photodissociation from man-made  $\text{CF}_x\text{Cl}_y$ . Figure 1 displays the altitude integral of these rates for three presumed time histories of  $\text{CF}_2\text{Cl}_2$  and  $\text{CFCl}_3$  (11): model 1, exponentially increasing with a doubling time of 3.5 years, the current pattern; model 2, exponential increase from 1960 to 1975, then constant at the 1975 rate; and model 3, exponential increase from 1960 to 1975, then immediate cessation. Figure 1 also presents globally integrated  $\text{O}_3$  destruction rates due to the chemical reactions of oxygen alone (labeled "Chapman") and for the  $\text{NO}_x$  catalytic cycles. These two  $\text{O}_3$  sinks are currently believed to control stratospheric  $\text{O}_3$  concentrations (8, 12). Models 1 and 2 yield rapidly increasing  $\text{O}_3$  destruction rates that will equal the natural sinks by about 1982 and 1986, respectively. Model 3 shows that, if  $\text{CF}_x\text{Cl}_y$  emissions were curtailed now, the ensuing  $\text{O}_3$  destruction rates would maximize around 1990 at a rate comparable to major natural cycles and would persist for several decades. Even larger effects may be possible because in our calculations we consider only the first chlorine atom released from each  $\text{CF}_x\text{Cl}_y$  molecule; in reality, all four halogen atoms may be freed (13).

Important parameters in calculations leading to Fig. 1 appear in Table 1. To account for vertical transport in our time-dependent, one-dimensional (altitude) model we adopted and smoothed the relatively high eddy diffusion coefficient ( $K$ ) profile of Wofsy and McElroy (14). To compute photodissociation coefficients,  $J$ , for  $\text{CF}_2\text{Cl}_2$  and  $\text{CFCl}_3$  we used available laboratory